A Novel Circularly Polarized Antenna With Coin-Shaped Patches and a Ring-Shaped Strip for Worldwide UHF RFID Applications

XiongYing Liu, *Member, IEEE*, Yi Liu, and Manos M. Tentzeris, *Fellow, IEEE*

***Abstract*—A circularly polarized radio frequency identification (RFID) reader antenna is presented for worldwide ultra- high frequency (UHF) applications. The antenna is composed of two coin-shaped patches, a ring-shaped strip, and a suspended feeding strip with open-circuited termination. The measurements show that the antenna has an impedance bandwidth ($S_{11} < -21$ dB) of 22.4% (768–962 MHz) and a stable gain with a peak value of 9.8 dBic. Moreover, it is immune to polarization mismatch with a 3-dB axial-ratio (AR) bandwidth of 15.9% (816–957 MHz) and a 3-dB AR beamwidth of more than 66°. The proposed antenna can be a candidate for universal RFID readers at the UHF band of 840–955 MHz. Due to the fact that the square holes in the center of the coin-shaped patches can embed one additional small antenna, the proposed antenna has the potential to be a dual- or tri-band combined RFID reader antenna, spanning both the conventional UHF and the ISM band of 2.45 or 5.8 GHz.**

***Index Terms*—Axial ratio (AR), broadband antenna, circularly polarized (CP), impedance matching, radio frequency identification (RFID), ultra-high frequency (UHF).**

I. Introduction

RADIO frequency identification (RFID) is a technology that can be used to identify any object carrying an electronic tag by electromagnetic waves [1]. Owing to the advantages of long detection range, fast reading speed, and high data transfer rate, passive RFID systems at ultra-high frequency (UHF) band are preferred in many applications, such as animal tagging, supply chain management, and electronic payment. However, the UHF frequencies authorized for RFID applications are particular in different countries and regions [2], e.g., 840.5–844.5 and 920.5–924.5 MHz allocated for China, 866–869 MHz for Europe, and 902–928 MHz for North and South America. Therefore, if the entire band of 840–955 MHz is covered, RFID systems will be universal with the advantages of simplified implementation and reduced cost.

As is known, typical RFID systems consist of readers and tags, and the tag antennas are normally linearly polarized. Considering the arbitrary orientation of the tags, circularly polarized (CP) antennas are selected in UHF RFID readers to avoid severe polarization mismatch between readers and tags [3]. CP antennas can be obtained by exciting two spatial orthogonal modes of equal amplitude with a 90° phase difference [4]. The design of CP antennas for RFID applications has been playing a crucial role in the continuous development of RFID technology. Up to now, various CP reader antennas for UHF RFID system have been studied. A planar reader antenna covering UHF band of 860–960 MHz is presented in [5] by insetting a grounded arc-shaped strip to a square slot and feeding with an F-shaped microstrip line. A crossed-dipole reader antenna with phase delay lines is designed in [6], which has a 3-dB axial-ratio (AR) band of 905–935 MHz. An aperture-coupled patch antenna for RFID readers with a Wilkinson power divider feeding network is realized in [7], whose 3-dB AR bandwidth is 909–921 MHz. The above-mentioned antennas either have a bidirectional radiation pattern or suffer from a narrow bandwidth, a low gain, and a complex feeding structure. Hence, some stacked patch antennas have been proposed [1], [4] to achieve broadband CP antenna configurations with high gain and simultaneously reach a compromise between performance and complexity.

Compared to the common square-shaped patch CP antenna [4], in this letter, a stacked coin-shaped patch CP antenna for UHF RFID applications is proposed. The antenna comprises two suspended coin-shaped patches, a ring-shaped strip, and a feeding strip. The main patch is sequentially fed by four probes, which are positioned along the feeding strip. A parasitic patch is positioned right above the main patch for broadening the bandwidth. In particular, the square holes in the center of the two patches, two slots on the diagonal of the main patch, and the ring-shaped strip along the edge of the parasitic patch are introduced to enhance the performance of S_{11} and AR.

II. Antenna Configuration

Fig. 1 shows the structure of the proposed antenna in detail. The antenna is composed of two radiating patches (i.e., the main patch and the parasitic one), a suspended feeding strip, a ring-shaped strip, and a finite-size ground plane. The feeding strip with a width of 26 mm is suspended above the ground plane (250×250 mm^2) at a height of $h1$. In order to improve

Manuscript received July 22, 2014; revised October 24, 2014; accepted November 19, 2014. Date of publication December 04, 2014; date of current version March 02, 2015. This work was supported in part by the National Natural Science Foundation of China under Grant 61372008, the Fundamental Research Funds for the Central Universities under Grant 2014ZZ0031, and the National Engineering Technology Research Center for Mobile Ultrasonic Detection.

X. Y. Liu and Y. Liu are with the School of Electronic and Information Engineering, South China University of Technology, Guangzhou 510640, China, and also with the State Key Laboratory of Millimeter Waves, Nanjing 210096, China (e-mail: liuxy@scut.edu.cn).

M. M. Tentzeris is with the School of Electrical and Computer Engineering, Georgia Institute of Technology, Atlanta, GA 30332 USA (e-mail: etentze@ece.gatech.edu).

Color versions of one or more of the figures in this letter are available online at http://ieeexplore.ieee.org.

Digital Object Identifier 10.1109/LAWP.2014.2378513

1536-1225 © 2014 IEEE. Personal use is permitted, but republication/redistribution requires IEEE permission.
See http://www.ieee.org/publications_standards/publications/rights/index.html for more information.

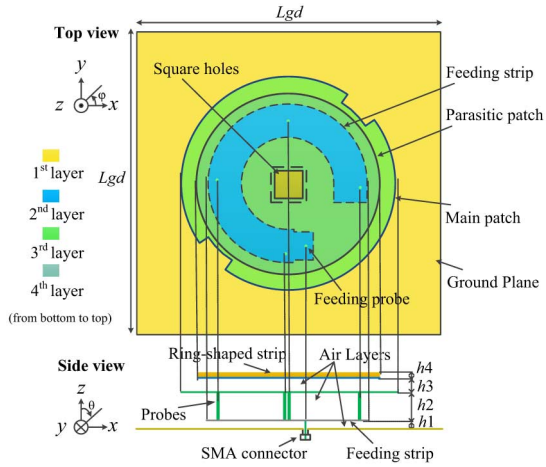

Fig. 1. Configuration of the proposed antenna.

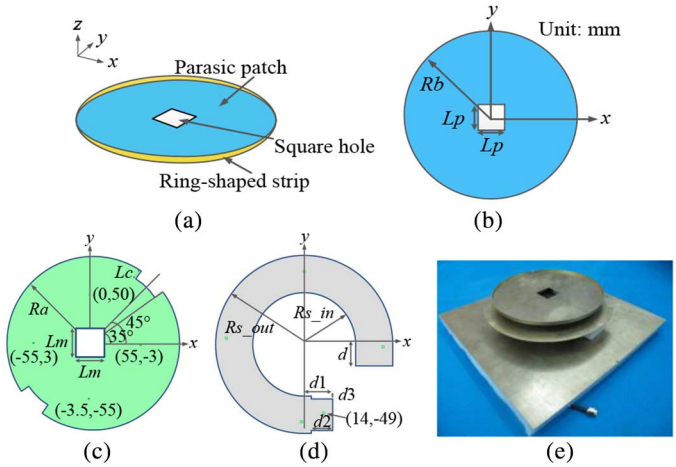

Fig. 2. Structures of (a) parasitic patch with ring-shaped strip, (b) parasitic patch, (c) main patch, (d) feeding strip, and (e) the prototype.

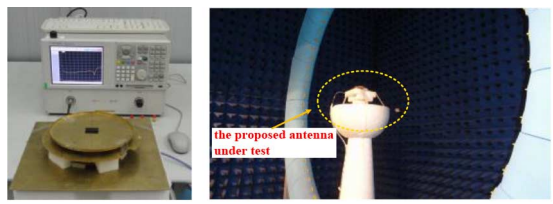

Fig. 3. Photographs of the experiment using (a) Agilent N5 230A vector network analyzer and (b) SATIMO near-field measurement system.

the impedance matching, two small slots are cut off at the signal input side of the feeding strip, increasing the input resistance and reactance in the operating band. According to previous studies [8], the thick air can act as substrate to enhance bandwidth and gain. The large inductance caused by the long probes can be effectively canceled out with the effect of the strong electromagnetic coupling between the feeding strip and the radiating patch [9]. This is one of the approaches to achieve a merit impedance matching and broaden the AR bandwidth.

Along this train of thought, a large spacing with a height of $h2$ between the feeding strip and the main patch with a radius of Ra is adopted. Two slots with a radian of 20° and a width of Lc are cut along the diagonal of the main patch to produce degenerate modes for widening the AR bandwidth. The main patch and the feeding strip are connected by four probes with a diameter of 2.2 mm, a size of which introduces a proper input resistance for a better impedance matching. Along the feeding strip, the physical length between any adjacent probes is about 83.3 mm, which equals to a quarter-wavelength at the center frequency of 900 MHz, corresponding to creating 90° phase difference between adjacent probes to achieve CP radiation. To further enhance the bandwidth, a parasitic patch with a radius of Rb is placed right above the main patch with a spacing of $h3$, contributing two local minimum axial ratio values. Two square holes are cut out with a dimension of $Lm \times Lm$ and $Lp \times Lp$ in the center of the main patch and the parasitic one, respectively, making the elements look like coins. The introduced holes can strengthen the coupling between the main and the parasitic patches that has a significant impact on the impedance matching and on the AR. In particular, a ring-shaped strip with a height of $h4$ is inlaid along the edge of parasitic patch, which has influence on the resistance part of the input impedance in the operating band. Through adjusting the geometric parameters of the proposed design with the aid of ANSYS HFSS ver. 13, we finally obtained the optimal dimensions of the antenna, as listed in Table I.

TABLE I
OPTIMAL DIMENSIONS OF THE PROPOSED ANTENNA

Symbol	Value (mm)	Symbol	Value (mm)
Lgd	250	*h*4	4
Ra	*90*	*Lc*	10.2
Rb	76	*Lm*	30
Rs_out	62	*Lp*	24
Rs_in	36	*d*	15
*h*1	5	*d*1	20
*h*2	20	*d*2	15
*h*3	10	*d*3	2

III. Results and Analysis

Fig. 2 shows the fabricated antenna topology and its individual parts with detailed dimensions. The S_{11} parameters, the AR, the gain, and the radiation patterns were measured for verification. The photographs of experimental setup are exhibited in Fig. 3.

A. Discussion About the Simulated and Measured Results

Based on our previous work [10], further research has been performed. Fig. 4 gives the simulated and measured performance of the antenna for comparison. With reference to Fig. 4(a), the band covering 768–962 MHz or with a fractional bandwidth of 22.4% is obtained with the measured reflection coefficient less than -21 dB. As shown in Fig. 4(b), the measured 3-dB AR bandwidth is about 141 MHz from 816–957 MHz or 15.9%, with a minimum axial ratio of 0.76 dB at 840 MHz. It can also be observed in Fig. 4(b) that the gain is stable with a maximum of 9.8 dBic within the operating bandwidth. However, some differences between the measured values and the simulated ones can be observed, mainly due to manufacturing tolerance, such as deformation of ground plane, the solder joints on the four probes and coaxial cable, and an unequal height of the four probes.

The surface current distributions at 915 MHz on the main patch are plotted in Fig. 5, demonstrating the directions of the distributed current at different time phase (t) from $0T$ to $3T/4$

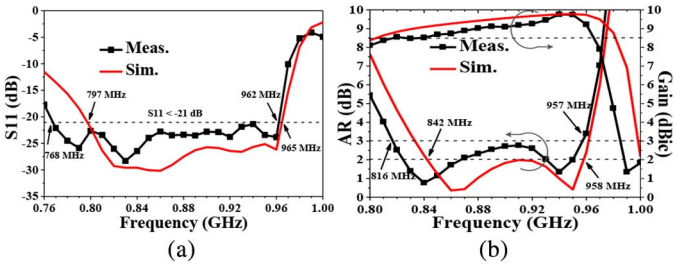

Fig. 4. Simulated and measured results of the proposed antenna: (a) S_{11}; (b) AR and gain.

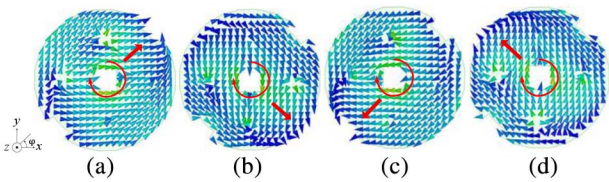

Fig. 5. Current distribution on the main patch at the different time: (a) $t = 0T$, (b) $t = T/4$, (c) $t = 2T/4$, and (d) $t = 3T/4$.

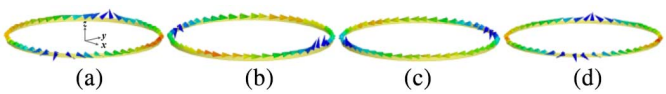

Fig. 6. Current distribution on the ring-shaped strip at (a) $t = 0T$, (b) $t = T/4$, (c) $t = 2T/4$, and (d) $t = 3T/4$.

with an interval of $T/4$, where T represents the period. It is obvious that the current on the main patch travels in the clockwise direction as t increases, exciting a left-hand circularly polarized (LHCP) radiation, i.e., copolarized radiation.

In the structure of the proposed antenna, the ring-shaped strip, which is inlaid along the edge of the parasitic patch, plays a crucial role in the radiation performance. Fig. 6 plots a "crown-like" current distribution on the ring-shaped strip at 915 MHz, recording the current diagram within one cycle. Observing the current flow directions, they are similar to those on the parasitic and main patches. According to the duality principle [11], the "crown-like" current distribution on the ring is equivalent to a magnetic dipole, which can improve the performance of S_{11}, AR, and radiation pattern.

Fig. 7 depicts the simulated and measured co- and cross-polarized radiation patterns at 840, 910, and 950 MHz, respectively, in the xz- and yz-planes. It is observed that the radiation patterns are almost symmetrical in both planes, and the 3-dB AR beamwidth is more than 66°, which is mainly benefited from the symmetry of the proposed antenna structure. In addition, although a finite-size ground plane is used, the front-to-back ratio is more than 15 dB at the entire operating band.

B. Effect of the Ring-Shaped Strip

We analyzed the effects of the ring-shaped strip on the S_{11} and AR by simulation. With reference to Fig. 8, it can be inferred that as $h4$ reduces from 5 to 3 mm, the impedance matching gets worse in the operating band, while the curves of AR are shifted up in higher frequency, mainly due to the expanding difference between the amplitudes ($|E_x|$, $|E_y|$) of the two orthogonal radiation fields E_x and E_y. When the ring-shaped strip is removed completely, the worst case of S_{11} and AR values is obvious. Finally, an optimal value of $h4 = 4$ mm is obtained. Thus, the

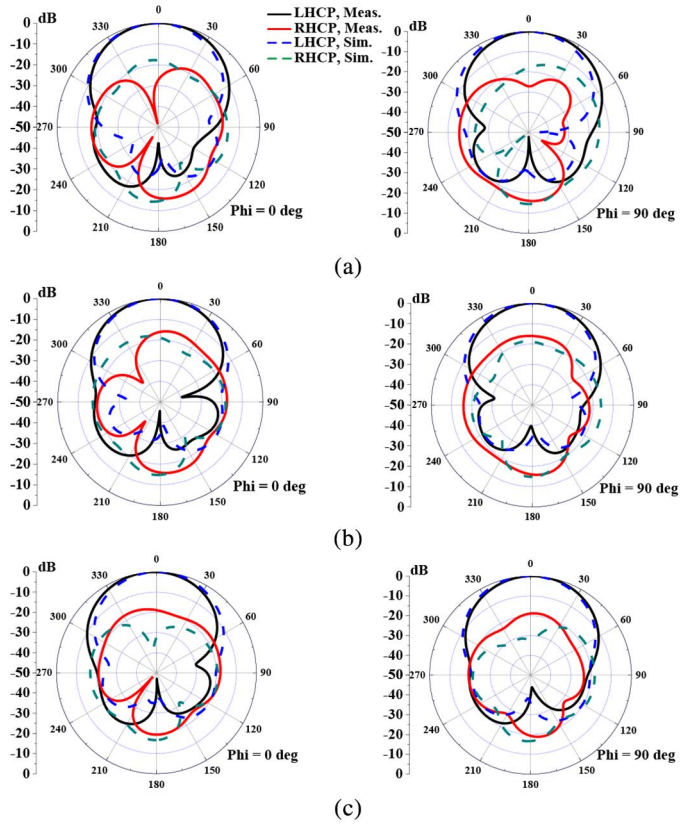

Fig. 7. Simulated and measured radiation patterns of the proposed antenna at (a) 840, (b) 910, and (c) 950 MHz.

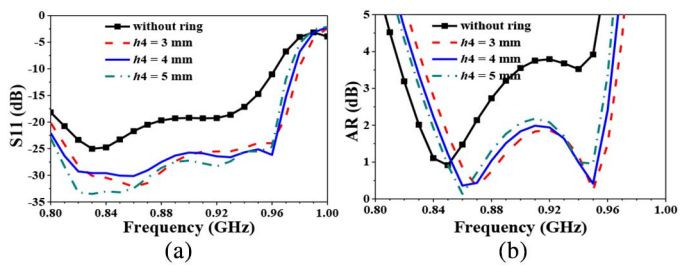

Fig. 8. Effect of the height of the ring-shaped strip on (a) S_{11} and (b) AR.

magnetic dipole is necessary to achieve a better performance of the proposed antenna.

C. Usefulness of the Square Hole in the Center of the Main Patch

As shown in Fig. 9, the square hole with different width of Lm introduced in the center of the main radiation patch has a severe impact on the performance of S_{11} and AR. However, also the square slot leaves available space for the setup of more electronic devices, such as an additional antenna. The initial UHF antenna can serve as a reflector for the additional small subantenna. Hence, a combined antenna [12], covering the universal UHF band of 840–960 MHz and the global ISM band of 2.45 or 5.8 GHz, can be constructed.

D. Robustness to Fabrication Inaccuracy

For saving computing time, perfect electric conductor (PEC) with a thickness of zero was assigned to the main and parasitic patches, ring-shaped strip, feeding strip, and ground plane

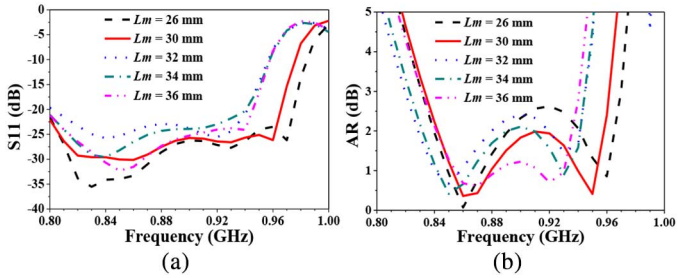

Fig. 9. Effect of the square hole in the center of the main patch on (a) S_{11} and (b) AR.

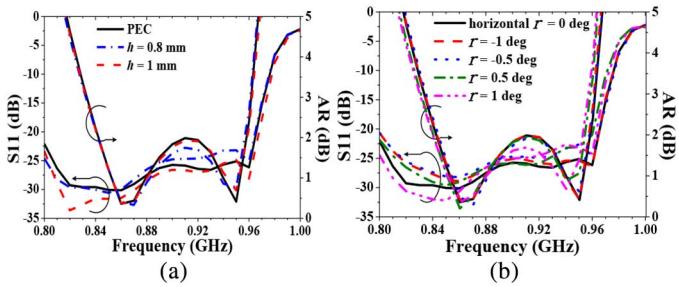

Fig. 10. Robustness under the conditions of (a) different copper thickness and (b) slope angles between main patch and horizontal xy-plane.

TABLE II
COMPARISON OF VARIOUS BROADBAND CP UHF RFID READER ANTENNAS

Refs.	S11	AR (3-dB)	Gain (dBic)
[1]	-14 dB, 25.8% 758-983 MHz	13.5% 838-959 MHz	8.6-8.8
[3]	-10 dB, 31.2% 828-1134 MHz	21.8% 845-1052 MHz	5-7.8
[4]	-14 dB, 22.0% 780-973 MHz	14.9% 830-964 MHz	8.3-9.3
[5]	-10 dB, 16.9% 846-1002 MHz	17.7% 857-1023 MHz	5.4-6.8
[13]	-10 dB, 10.6% 870-967 MHz	6% 893-948 MHz	8.5-8.9
Proposed Antenna	-21 dB, 19.1% 797-965 MHz	14.4% 833-962 MHz	9.1-9.8

in HFSS simulation. However, during the practical fabrication, the copper with a thickness of $h = 1$ mm was adopted. With reference to Fig. 10(a), the divergence can be acceptable when copper is thin enough. Moreover, due to fabrication tolerance, the real heights of the four probes may be uneven, making a slope between the main patch and horizontal xy-plane with an angle of r. As demonstrated in Fig. 10(b), a small slant has almost no influence on the performance of the proposed antenna.

E. Comparison of Performance

A performance comparison between four previously published sets of antennas for UHF RFID readers and our proposed antenna is made in Table II. We considering some uncertain factors in terms of manufacturing process, so only the simulated values are summarized.

Here, it is pointed out that if the proposed antenna performance is permitted to slightly degrade in the operating band, an even wider bandwidth can be achieved. Hence, a reasonable tradeoff can be made between performance and bandwidth.

IV. CONCLUSION

In this letter, a broadband CP stacked coin-shaped patch antenna for a universal UHF RFID reader has been presented. During the process of design, a tradeoff between performance enhancement and structure simplification was made. To achieve circular polarization, the main patch is fed by four probes, which are connected to the feeding strip with an interval of a quarter-wavelength at 900 MHz. Through experimental and theoretical analysis, we find that the ring-shaped strip inlaid along the edge of parasitic patch has a significant effect on the performance of the impedance matching and AR. Moreover, the square holes introduced in the center of the main patch and the parasitic one can not only enhance the coupling between the two patches, but also leave space for additional electronic devices setup, such as one more multifrequency antenna. The measured results show that the proposed antenna has an impedance bandwidth ($S_{11} < -21$ dB) of 22.4% or 768–962 MHz, a 3-dB AR bandwidth of 15.9% or 816–957 MHz, a 3-dB AR beamwidth of more than 66°, a stable gain with average level of 9.1 dBic, and a front-to-back ratio of at least 15 dB in the whole bandwidth. Therefore, the proposed CP antenna has the potential use in high-performance global-operability UHF readers for long-range identification and wide-coverage applications.

REFERENCES

[1] Z. Wang, S. Fang, S. Fu, and S. Jia, "Single-fed broadband circularly polarized stacked patch antenna with horizontally meandered strip for universal UHF RFID applications," *IEEE Trans. Microw. Theory Tech.*, vol. 59, no. 4, pp. 1066–1073, Apr. 2011.

[2] Nasimuddin, Z. N. Chen, and X. Qing, "Asymmetric-circular shaped slotted microstrip antennas for circular polarization and RFID applications," *IEEE Trans. Antennas Propag.*, vol. 58, no. 12, pp. 3821–3828, Dec. 2010.

[3] E. Mireles and S. K. Sharma, "A novel wideband circularly polarized antenna for worldwide UHF band RFID reader applications," *Prog. Electromagn. Res. B*, vol. 42, pp. 23–44, Jun. 2012.

[4] Z. N. Chen, X. Qing, and H. L. Chung, "A universal UHF RFID reader antenna," *IEEE Trans. Microw. Theory Tech.*, vol. 57, no. 5, pp. 1275–1282, May 2009.

[5] J. H. Lu and S. F. Wang, "Planar broadband circularly polarized antenna with square slot for UHF RFID reader," *IEEE Trans. Antennas Propag.*, vol. 61, no. 1, pp. 45–53, Jan. 2013.

[6] Y. F. Lin, Y. K. Wang, H. M. Chen, and Z. Z. Yang, "Circularly polarized crossed dipole antenna with phase delay lines for RFID handheld reader," *IEEE Trans. Antennas Propag.*, vol. 60, no. 3, pp. 1221–1227, Mar. 2012.

[7] D. Yu, Y. Ma, Z. Zhang, and R. Sun, "A circularly polarized aperture coupled patch antenna for RFID reader," in *Proc. 4th WiCOM*, Dalian, China, 2008, pp. 1–3.

[8] F. S. Chang, K. L. Wong, and T. W. Chiou, "Low-cost broadband circularly polarized patch antenna," *IEEE Trans. Antennas Propag.*, vol. 51, no. 10, pp. 3006–3009, Oct. 2003.

[9] Z. Wang, S. Fang, S. Fu, and X. Li, "Circularly polarized antenna with U-shaped strip for RFID reader operating at 902–928 MHz," in *Proc. Signals Syst. Electron. Int. Symp.*, Nanjing, China, 2010, pp. 1–3.

[10] Y. Liu and X. Y. Liu, "Circularly polarized antenna with circular shaped patch and strip for worldwide UHF RFID applications," in *Proc. Antennas Propag. Int. Symp.*, Nanjing, China, 2013, pp. 1154–1157.

[11] C. A. Balanis, *Antenna Theory: Analysis and Design*, 3rd ed. New York, NY, USA: Wiley, 2005.

[12] J. Anguera, E. M. Ortigosa, C. Puente, C. Borja, and J. Soler, "Broadband triple-frequency microstrip patch radiator combining a dual-band modified Sierpinski fractal and a monoband antenna," *IEEE Trans. Antennas Propag.*, vol. 54, no. 11, pp. 3367–3373, Nov. 2006.

[13] X. Chen, G. Fu, S. X. Gong, Y. L. Yan, and W. Zhao, "Circularly polarized stacked annular-ring microstrip antenna with integrated feeding network for UHF RFID readers," *IEEE Antennas Wireless Propag. Lett.*, vol. 9, pp. 542–545, 2010.